Temperature Dependence of the Diffusive Conductivity for Monolayer and Bilayer Graphene

Shaffique Adam and M. D. Stiles

Center for Nanoscale Science and Technology, National Institute of
Standards and Technology, Gaithersburg, Maryland 20899-6202, USA
(Dated: December 9, 2009)

Assuming diffusive carrier transport, and employing an effective medium theory, we calculate the temperature dependence of the conductivity due to Fermi surface broadening as a function of carrier density for both monolayer and bilayer graphene. We find that the temperature dependence of the conductivity depends strongly on the amount of disorder. The conductivity is a function of T/T^*, where T^* is the characteristic temperature set by the disorder. For bilayer graphene, our results are in good quantitative agreement with recent experiments.

Monolayer and bilayer graphene are distinct electronic materials. Monolayer graphene is a sheet of carbon in a honeycomb lattice that is one atom thick, while bilayer graphene comprises two such sheets, each in a honeycomb lattice, with the first lattice 0.3 nm above the second. Since the first transport measurements [1] in 2005, we have come a long way in understanding the basic transport mechanisms of carriers in these new carbon allotropes.

At low energies relevant for most experiments, monolayer graphene has a linear dispersion while bilayer graphene has a parabolic dispersion. A unique feature of graphene is that the density of carriers can be tuned continuously by an external gate from electron-like carriers at positive doping to holes at negative doping [2].

At precisely zero doping, in the absence of any disorder and at zero temperature, there are no free carriers. One expects ballistic transport through evanescent modes to give rise to a universal conductivity in both monolayer [3] and bilayer graphene [4]. In practice, one is in the "ballistic regime" so long as the disorder-limited mean-free path is larger than the distance between the contacts [5].

For monolayer graphene at finite temperature, the thermal smearing of the Fermi surface gives a density $n(T) \sim T^2$. For ballistic transport in these monolayers, the conductivity $\sigma \sim \sqrt{|n|}$ for large n, so $\sigma(T) \sim T$ [6]. Indeed, it was recently shown [7] that in the absence of disorder, $\sigma(T)$ interpolates from the universal $\sigma_{\min}$ to the linear in T regime following a function that depends only on T/T_{F}; (T_{F} is the Fermi temperature).

However, it seems that the vast majority of experiments on graphene are in the dirty limit, where the carrier transport is diffusive [8]. The characteristic features of this regime are a conductivity for both monolayer and bilayer graphene that is linear in density (i.e. $\sigma = ne\mu_c$, with a mobility μ_c that is independent of temperature and carrier density [9, 10]), and the existence of a minimum conductivity plateau in $\sigma(n)$, with $\sigma_{\min} = n_{\mathrm{rms}}e\mu_c/\sqrt{3}$ [11]. n_{rms} is the root-mean-square fluctuation in carrier density induced by the disorder.

The purpose of the current work is to address the question: What is the temperature dependence of this minimum conductivity plateau for both monolayer and bilayer graphene in the presence of disorder?

This problem is complicated by the fact that in regions of inhomogeneous carrier density (i.e. puddles of electrons and holes) induced by the disorder, there will be activation of both electron and hole carriers at finite temperature. Moreover, the ratio between electron-puddles and hole-puddles changes continuously with carrier density, until at very high density there is only a single type of carrier.

The temperature dependence of the conductivity in the limit of high density with only a single carrier was considered in Ref. [12]. Reference [10] modeled the temperature dependence of the Dirac point conductivity by assuming that the graphene samples comprised just two big "puddles" each with the same number of carriers. In the appropriate limits, our results agree with these previous works. Here we provide a semi-analytic expression for the graphene conductivity by averaging over the random distribution of puddles with different carrier densities. This result is valid throughout the crossover from the Dirac point (where fluctuations in carrier density dominate) to high density (where these fluctuations are irrelevant), both with and without the thermal activation of carriers.

Given a microscopic model for the disorder, one could compute both μ_c and n_{rms} [13]. Alternatively, μ_c could be determined from low temperature transport measurements and n_{rms} from local probe measurements [14]. In what follows, we take μ_c and n_{rms} to be parameters of the theory. As a consequence, the results reported here do not depend on the microscopic details of the impurity potential, provided it is reasonably well characterized by this parameterization.

The key assumption in this work is the applicability of Effective Medium Theory (EMT), which describes the bulk conductivity σ_{EMT} of an inhomogeneous medium by

the integral equation [15]

$$\int dn P[n] \frac{\sigma(n) - \sigma_{\text{EMT}}}{\sigma(n) + \sigma_{\text{EMT}}} = 0. \quad (1)$$

$P[n]$ is the probability distribution of the carrier density in the inhomogeneous medium – positive (negative) n corresponds to (electrons) holes, and $\sigma(n)$ is the local conductivity of a small patch with a homogeneous carrier density n. Ignoring the denominator, Eq. 1 gives the average conductivity. The denominator correctly weights the integral to cancel the build-up of any internal electric fields. The validity of this approximation for monolayer graphene was shown to be good in Refs. [15–17]. In Ref. [16], for example, it was shown that for sufficiently large disorder the transport is semiclassical and quantum corrections and any additional resistance caused by the $p-n$ interfaces between the electron and hole puddles can be ignored. Since we are concerned with diffusive transport in the dirty limit, we assume that the EMT results hold for both monolayer and bilayer graphene.

We derive a semi-analytic equation for effective medium conductivity σ_{EMT} from Eq. 1 using two assumptions: First, we assume that the distribution function $P[n, n_g]$ is Gaussian [18] centered at n_g, (i.e. the field effect carrier density induced by the back gate and assumed to be proportional to V_g), with width n_{rms}. Second, we write the local conductivity as $\sigma(n, T) = n_{\text{rms}} e \mu_c H(z, t)$. Below we will calculate the dimensionless function $H(z, t)$ assuming thermally activated carrier transport with constant n_{rms} and μ_c and show that it depends only on scaled variables $z = n/n_{\text{rms}}$ and $t = T/T^*$. Here, using the definitions $z_g = n_g/n_{\text{rms}}$, $\bar{\sigma}[z_g, t] = \sigma_{\text{EMT}}/(n_{\text{rms}} e \mu_c)$, $T^* = \hbar v_{\text{F}} \sqrt{\pi n_{\text{rms}}}$ for monolayer graphene and $T^* = \pi \hbar^2 n_{\text{rms}}/2m$ for bilayer graphene, (with $h = 2\pi\hbar$ is Planck's constant), we manipulate Eq. (1) into a dimensionless form

$$\int_0^\infty dz \exp\left[-z^2/2\right] \cosh\left[z_g z\right] \frac{H[z, t] - \bar{\sigma}[z_g, t]}{H[z, t] + \bar{\sigma}[z_g, t]} = 0. \quad (2)$$

With the analytical results for $H(z, t)$ discussed below, this implicit equation can be solved either perturbatively or by numerical integration to give σ_{EMT}.

Equation 2 correctly reproduces various known limits. For example, in the limit $T \to 0$ (where $H[z, 0] = z$), the results of Ref. [19] are reproduced for $n_g \gg n_{\text{rms}}$, and the results of Ref. [11, 15] are reproduced for $n_{\text{rms}} \gg n_g$. For $T = 0$, we find $\sigma_{\min} \approx n_{\text{rms}} e \mu_c / \sqrt{3}$ for both monolayer and bilayer graphene. In the limit $T \gg T_{\text{F}}$, $n_g \gg n_{\text{rms}}$, we obtain the results of Ref. [12], while for $T \gg T^*$, $H[z, t]$ is independent of z giving (for any gate voltage) the solutions $\bar{\sigma} = \pi^2 t^2/3$ for monolayer and $\bar{\sigma} = 2t \ln 2$ for bilayer graphene.

A consequence of Eq. 2 is that the amount of disorder in the sample sets the scale for the temperature depen-
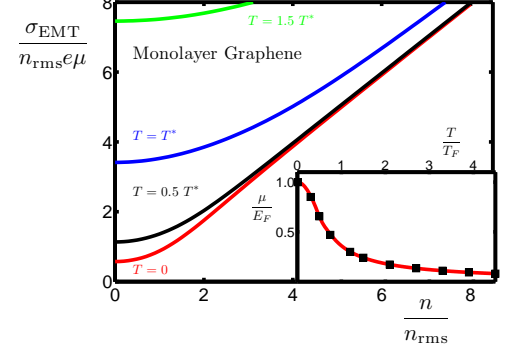

FIG. 1: (Color online) Monolayer graphene conductivity as a function of temperature and carrier density. From bottom to top, the curves are for $T/T^* = 0, 0.5, 1$, and 1.5, where T^* is a characteristic temperature scale set by the amount of disorder. Due to the large T^* in monolayer graphene, most experiments would probe the regime $T/T^* \lesssim 0.5$. Inset: Monolayer chemical potential as a function of temperature. Solid line shows the interpolation function (Eq. 4).

dence i.e. $T/T^* \approx 1$ separates the low temperature behavior, where the magnitude of the conductivity and its temperature dependence are set by the disorder, from the high temperature limit where the conductivity from thermally excited carriers dominate the transport ($\sigma \sim T^2$ for monolayer graphene and $\sigma \sim T$ for the bilayer independent of both gate voltage and disorder). Our result explains the empirical observations of Ref. [20], where the saturation in the temperature dependence of the conductivity was found to be correlated with the sample quality.

To proceed we need to calculate the function $H(z, t)$. For thermal activation of carriers, the chemical potential μ is determined by solving for $n_g = n_e - n_h$ [12], where

$$n_e(T) = \int_0^\infty dE \, D(E) f(E, \mu, k_{\text{B}} T),$$

$$n_h(T) = \int_{-\infty}^0 dE \, D(E) \left[1 - f(E, \mu, k_{\text{B}} T)\right], \quad (3)$$

where $f(E, \mu, k_{\text{B}} T)$ is the Fermi-Dirac function and k_{B} is the Boltzmann constant. The density of states for monolayer graphene is $D(E) = 2|E|/(\pi \hbar^2 v_{\text{F}}^2)$, while for bilayer graphene at low density, $D(E) = 2m/\pi \hbar^2$. For $T = 0$, only majority carriers are present, while for $T \to \infty$ activated carriers of both types are present in equal number.

For the crossover regime, we have $n_{e(h)} = -2n_g(T/T_{\text{F}})^2 \text{Li}_2\left[-\exp(\mp\mu/k_{\text{B}} T)\right]$ for monolayer graphene, where $\text{Li}_2(z) = \int_z^0 dt \, t^{-1} \ln(1 - t)$ is the dilogarithm function. Data points in the inset of Fig. 1 show chemical potential $\mu(T)$ obtained by the numerical solution of the implicit equation, $1 =$
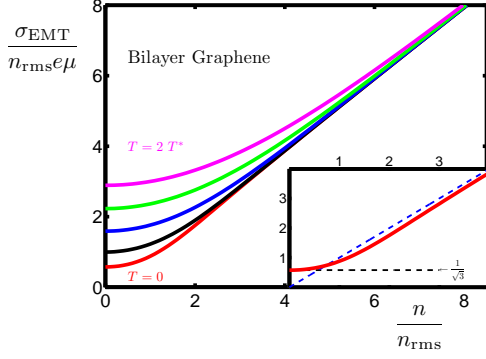
FIG. 2: (Color online) Bilayer layer graphene conductivity as a function of temperature and carrier density for $T/T^* = 0, 0.5, 1, 1.5,$ and 2. Inset shows a close-up of the zero temperature minimum conductivity (which is the same for both monolayer and bilayer graphene). The dashed horizontal line shows the result of Ref. [11] and the other dashed line is the high-density transport result of Ref. [19]. The solid line (Eq. 2) captures the full crossover from the regime where the conductivity is dominated by the disorder induced carrier density fluctuations, to the semiclassical Boltzmann transport regime.
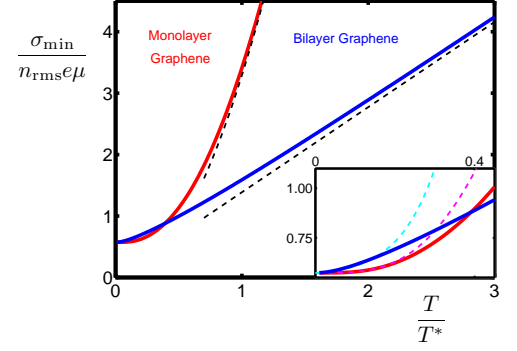

FIG. 3: (Color online) Minimum conductivity as a function of temperature for monolayer (upper curve) and bilayer (lower curve) graphene. Dashed lines show the high temperature asymptotes $\sigma_{\min} \to \pi e \mu_c T^2 / (3\hbar^2 v_{\mathrm{F}}^2)$ for monolayer and $\sigma_{\min} \to m e \mu_c 4 \ln 2 T / (\pi \hbar^2)$ for bilayer graphene. Inset: low density regime with perturbative results $\bar{\sigma}(t)/\bar{\sigma}(0) = 1 + 4\pi^2 t^4 \ln t / (9|\pi - 2|)$ for monolayer and $1 + 7.27 \times [t^2 - 2\sqrt{3} t^3 + 16 t^4]$ for bilayer graphene.

$2(T/T_{\mathrm{F}})^2 \{\mathrm{Li}_2[-\exp(\mu/k_{\mathrm{B}}T)] - \mathrm{Li}_2[-\exp(-\mu/k_{\mathrm{B}}T)]\}$, as well as the interpolation function

$$F_\mu(x) = \mu(T/T_{\mathrm{F}})/E_{\mathrm{F}} = g(x)(1 - \pi^2 x^2/6) + \bar{g}(x)/(4 \ln 2x), \quad (4)$$

where E_{F} is the Fermi energy, and $g(x) + \bar{g}(x) = 1$ are a choice of complementary functions, e.g. we use $g(x) = (1 + \mathrm{Erf}[10(x - 1/2)])/2$ and $\bar{g}(x) = \mathrm{Erfc}[10(x - 1/2)]/2$ [21]. Similarly, for bilayer graphene we find $n_{e(h)} = n_g(T/T_{\mathrm{F}}) \ln[1 + \exp(\mp\mu/k_{\mathrm{B}}T)]$ and $\mu = E_{\mathrm{F}}$. Using $\sigma(n, T) = (n_e + n_h)e\mu_c$, we find

$$H(z, t) = \begin{cases} \frac{\pi^2 t^2}{3} + z \left[F_\mu\left(\frac{t}{\sqrt{z}}\right) \right]^2, & \text{Monolayer} \\ z + 2t \ln\left[1 + e^{-z/t}\right], & \text{Bilayer.} \end{cases} \quad (5)$$

Figure 1 shows results for monolayer graphene. For a typical disorder of $n_{\mathrm{rms}} = 10^{11}$ cm^{-2}, $T^* \approx 475$ K. For high temperature, phonon scattering dominates the transport. Therefore, the regime relevant to experiments is between the red and black curves which show very weak temperature dependence. This is in sharp contrast to bilayer graphene (shown in Fig. 2), where for the same amount of disorder, $T^* \approx 40$ K and one can observe the full range of temperature dependence shown in the figure. We now focus on the minimum conductivity $\sigma_{\min}(T)$. Figure 3 shows a numerical solution for $\sigma_{\min}(T)$ as well as analytic asymptotes for both low and high temperature [26].

In Fig. 4 we compare the theory with several experiments in the literature. In principle, the two parameters of the theory μ_c and n_{rms} can be determined by looking at the gate voltage dependence of the low tem-
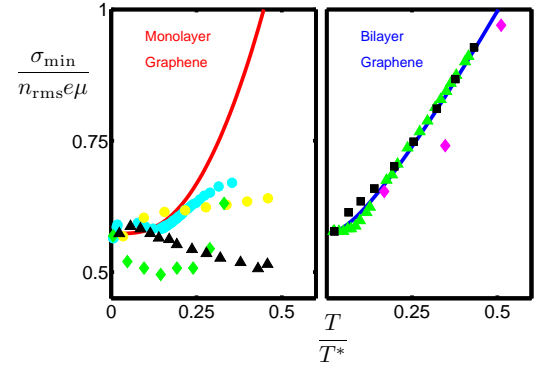

FIG. 4: (Color online) Same results as in Fig. 3 showing comparison with experimental data. Left panel shows monolayer graphene where circles are the two suspended samples (with $\mu_c = 1$ m^2/Vs, $T^* = 1080$ K and $\mu_c = 2.8$ m^2/Vs, $T^* = 170$ K) of Ref. [22] before annealing. (After annealing, these suspended samples did not show signatures of diffusive transport). Triangles (Ref. [23]) and Diamonds (Ref. [10]) are non-suspended devices with $\mu_c = 1.5$ m^2/Vs, $T^* = 720$ K and $\mu_c = 0.4$ m^2/Vs, $T^* = 1040$ K respectively. For all these samples, we use the value of low temperature mobility reported by the authors. Right panel shows bilayer graphene. Green triangles show suspended bilayer data from Ref. [20] using $\mu_c = 1.4$ m^2/Vs and $T^* = 36$ K. Black squares (Ref. [24]) and diamonds (Ref. [10]) are bilayers on a SiO$_2$ substrate with $\mu_c = 0.11$ m^2/Vs, $T^* = 530$ K and $\mu_c = 0.045$ m^2/Vs and $T^* = 290$ K. We were unable to obtain good agreement with the four data points of Ref. [9] using their reported value for the low temperature mobility. The apparent lack of correlation between n_{rms} and T^* for bilayer graphene suggests that multiple scattering mechanisms are at play [25].

perature conductivity, $\sigma(n_g, T \to 0)$. This fixes both $\sigma_{\min}[T = 0] \approx n_{rms}e\mu_c/\sqrt{3}$ and $T^*[n_{rms}]$ and therefore any agreement between theory and experiment (even for $T \gg T^*$) is significant. Where possible, we used the values of low temperature mobility μ_c reported in the literature. However, even without using the low temperature data to fix the parameters of the theory, the scaling of the conductivity $\sigma(T)$ in the crossover region $T/T^* \approx 1$ is non-trivial.

Bilayer graphene (right panel of Fig. 4) shows quantitative agreement with the theory. For monolayer graphene (left panel), the non-monotonicity in the experimental data suggest physics beyond the thermal activation of carriers considered here. In retrospect, this disagreement is not surprising. For dirty samples T^* is large, and since phonons degrade the mobility for $T \gtrsim 200\ K$, the theory is only valid for $t \ll 1$, where the effects of temperature dependent screening are strongest [27]. For clean samples, although T^* is small, the mean-free path is long and the transport becomes ballistic. For both ballistic samples, and for $t \ll 1$ one expects the conductivity to first decrease with increasing temperature [7, 12] before Fermi smearing reverses this trend. In contrast, the comparatively low T^* for bilayer graphene suggests that we capture the regime relevant to experiments.

In summary, we have developed an effective medium theory that captures the gate voltage and temperature dependence of the conductivity for both monolayer and bilayer graphene. The theory depends on two parameters: n_{rms} that sets the scale of the disorder, and μ_c the carrier mobility. Our main finding is that (except at very high temperature), disorder sets the scale for the temperature dependence, implying that the $\sigma(T)$ is yet another probe of the microscopic disorder. Our results show good agreement with the observed temperature dependence taken from bilayer experiments in the literature, suggesting that even some suspended samples are still the the diffusive (rather than ballistic) regime.

[1] K. S. Novoselov, A. K. Geim, S. V. Morozov, D. Jiang, Y. Zhang, M. I. Katsnelson, I. V. Grigorieva, S. V. Dubonos, and A. A. Firsov, Nature **438**, 197 (2005); Y. Zhang, Y.-W. Tan, H. L. Stormer, and P. Kim, Nature **438**, 201 (2005).

[2] A. H. Castro Neto, F. Guinea, N. M. R. Peres, K. S. Novoselov, and A. K. Geim, Rev. Mod. Phys. **81**, 109 (2009).

[3] M. I. Katsnelson, Eur. Phys. J. B **51**, 157 (2006); J. Tworzydło, B. Trauzettel, M. Titov, A. Rycerz, and C. W. J. Beenakker, Phys. Rev. Lett. **96**, 246802 (2006).

[4] I. Snyman and C. Beenakker, Phys. Rev. B **75**, 045322 (2007); J. Cserti, Phys. Rev. B **75**, 033405 (2007).

[5] F. Miao, S. Wijeratne, Y. Zhang, U. Coskun, W. Bao, and C. Lau, Science **317**, 1530 (2007); R. Danneau, F. Wu, M. F. Craciun, S. Russo, M. Y. Tomi, J. Salmilehto, A. F. Morpurgo, and P. J. Hakonen, Phys. Rev. Lett. **100**, 196802 (2008).

[6] X. Du, I. Skachko, A. Barker, and E. Andrei, Nature Nanotechnology **3**, 491 (2008).

[7] M. Müller, M. Bräuninger, and B. Trauzettel, Phys. Rev. Lett. **103**, 196801 (2009).

[8] For a review of the diffusive regime, see S. Adam *et al.* Solid State Commun. **149**, 1072 (2009) and J.-H. Chen *et al. ibid.* **149**, 1080 (2009), and references therein.

[9] S. V. Morozov, K. S. Novoselov, M. I. Katsnelson, F. Schedin, D. C. Elias, J. A. Jaszczak, and A. K. Geim, Phys. Rev. Lett. **100**, 016602 (2008).

[10] W. Zhu, V. Perebeinos, M. Freitag, and P. Avouris, Phys. Rev. B **80**, 235402 (2009).

[11] S. Adam, E. H. Hwang, V. M. Galitski, and S. Das Sarma, Proc. Natl. Acad. Sci. USA **104**, 18392 (2007).

[12] E. H. Hwang and S. Das Sarma, Phys. Rev. B **79**, 165404 (2009).

[13] For monolayer graphene, if corrugations are important, n_{rms} could be estimated from E. Kim and A. Castro Neto, EPL **84**, 57007 (2008), and μ_c from M. Katsnelson and A. Geim, Phil. Trans. R. Soc. A **366**, 195 (2008); whereas for charged impurities, $\mu_c[m^2/Vs] = 50/n_{imp}[10^{10}\ cm^{-2}]$, and Ref. [11] gives n_{rms} as an analytic function of n_{imp} and d, the distance of the impurities from the graphene sheet. A density functional approach was used by E. Rossi and S. Das Sarma, Phys. Rev. Lett. **101**, 166803 (2008) and M. Polini *et. al*, Phys. Rev. B **78**, 115426 (2008) to obtain n_{rms} numerically.

[14] J. Martin, N. Akerman, G. Ulbricht, T. Lohmann, J. H. Smet, K. von Klitzing, and A. Yacobi, Nature Physics **4**, 144 (2008); A. Deshpande, W. Bao, F. Miao, C. N. Lau, and B. J. LeRoy, Phys. Rev. B **79**, 205411 (2009); Y. Zhang, V. Brar, C. Girit, A. Zettl, and M. Crommie, Nature Physics **5**, 722 (2009); D. Miller, K. Kubista, G. Rutter, M. Ruan, W. de Heer, P. First, and J. Stroscio, Science **324**, 924 (2009).

[15] E. Rossi, S. Adam, and S. Das Sarma, Phys. Rev. B **79**, 245423 (2009).

[16] S. Adam, P. W. Brouwer, and S. Das Sarma, Phys. Rev. B **79**, 201404 (2009).

[17] M. M. Fogler, Phys. Rev. Lett. **103**, 236801 (2009).

[18] At the Dirac point, there is no significant difference [15] between the EMT conductivity results for Gaussian $P[n]$ and a numerical computation of $P[n]$ using a density functional theory with a microscopic disorder model.

[19] T. Ando, J. Phys. Soc. Jpn. **75**, 074716 (2006); E. H. Hwang, S. Adam, and S. Das Sarma, Phys. Rev. Lett. **98**, 186806 (2007).

[20] B. Feldman, J. Martin, and A. Yacoby, Nature Physics (advance online publication) 10.1038/nphys1406 (2009).

[21] I. S. Gradshteyn and I. M. Ryzhik, *Table of integrals, series, and products* (Academic Press, 1994), 5th ed.

[22] K. I. Bolotin, K. J. Sikes, J. Hone, H. L. Stormer, and P. Kim, Phys. Rev. Lett. **101**, 096802 (2008).

[23] J. H. Chen, C. Jang, S. Xiao, M. Ishigami, and M. S. Fuhrer, Nature Nanotechnology **3**, 206 (2008).

[24] M. Fuhrer, private communication (2009).

[25] After completion of this work, we received a copy of Das Sarma et al. arXiv:0912.0403, who using microscopic models show that both long-range and short-range scat-

terers are necessary to get the constant μ_c as observed experimentally. They also show that different scattering mechanisms affect T^* and μ_c differently.

[26] Analytic results in perturbation theory were obtained using a Lorentzian for $P[n]$. See discussion in Ref. [15].

[27] The effects of phonons that are important at high temperature [23] could be included by modifying $\sigma(n,T)$ using Matthiessen's rule. Since electronic screening depends on temperature, $n_{\rm rms}$ and μ_c depend weakly on T and n_g. This effect is important only for $T \ll T_{\rm F}$ [12]. Since Eq. 2 depends on the ratios $n_g/n_{\rm rms}$ and $\sigma_{\rm EMT}/ne\mu_c$, if $n_{\rm rms}(v_g, T)$ and $\mu_c(T)$ are known, their effects could be included by scaling the results presented here.